

1 **Supplementary Information**

2 **For**

3 **Porcine gut microbiota in mediating host metabolic adaptation to**
4 **cold stress**

5
6 **Yu Zhang^{1,2,3+}, Lan Sun^{1,2,3+}, Run Zhu^{1,2,3}, Shiyu Zhang^{1,2,3}, Shuo Liu^{1,2,3}, Yan**
7 **Wang^{1,2,3}, Yinbao Wu^{1,2}, Sicheng Xing^{1,2,3}, Xindi Liao^{1,2,3*}, Jiandui Mi^{1,2,3*}**

8
9 ¹ Guangdong Laboratory for Lingnan Modern Agriculture, South China Agricultural
10 University, Guangzhou 510642, China

11 ² National Engineering Research Center for Breeding Swine Industry, College of
12 Animal Science, South China Agricultural University, Guangzhou 510642, China

13 ³ Guangdong Provincial Key Lab of Agro-Animal Genomics and Molecular Breeding
14 and Key Lab of Chicken Genetics, Breeding and Reproduction, Ministry of Agriculture,
15 Guangzhou 510642, China

16 ⁺These authors contributed equally to this work.

17 ^{*} Corresponding author: Dr. Xindi Liao and Dr. Jiandui Mi.

18 Tel: 86-20-85280279, Fax: 86-20-85280740, E-mail address: xdliao@scau.edu.cn;

19 mijiandui@163.com, Full postal address: College of Animal Science, South China

20 Agricultural University, Wushan Road, Tianhe District, Guangzhou, 510642, P. R.

21 China

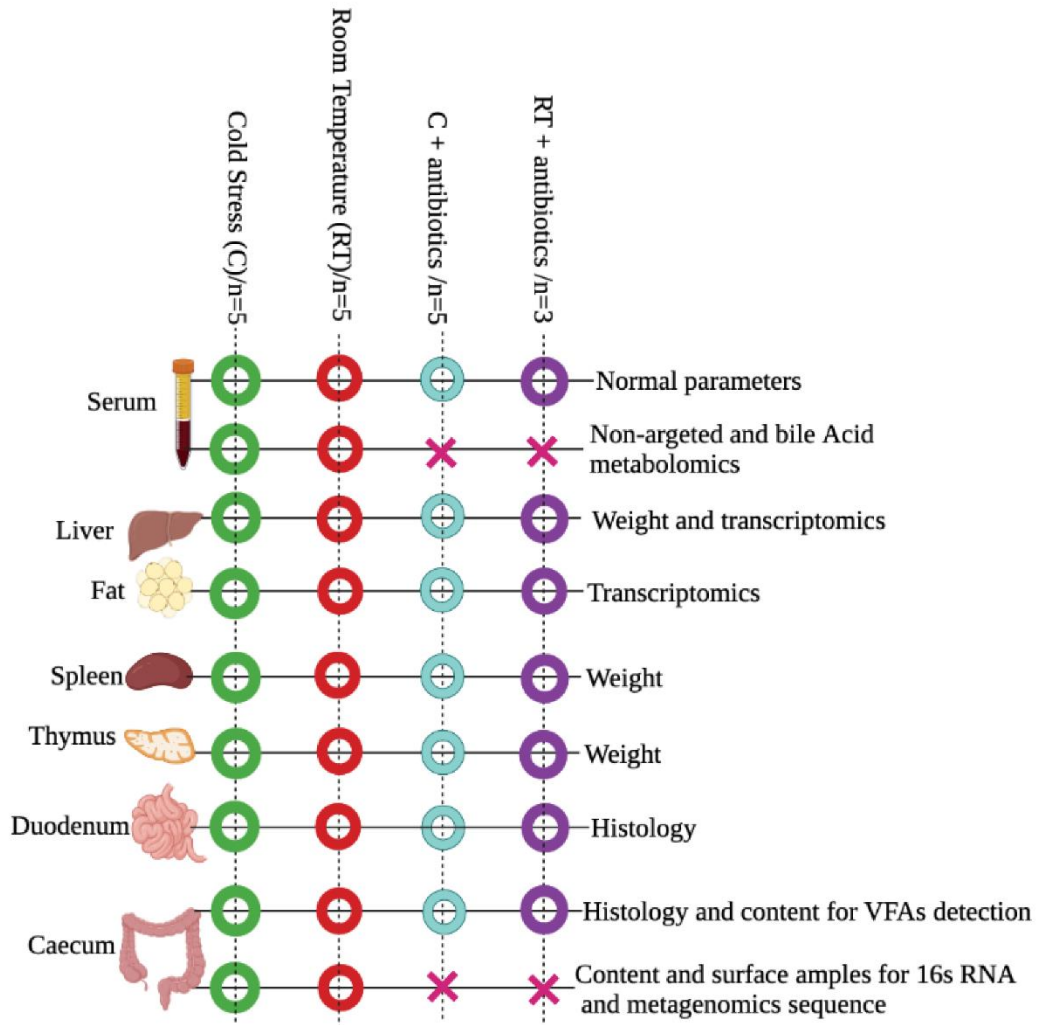
22

23

24
25
26
27

Contents

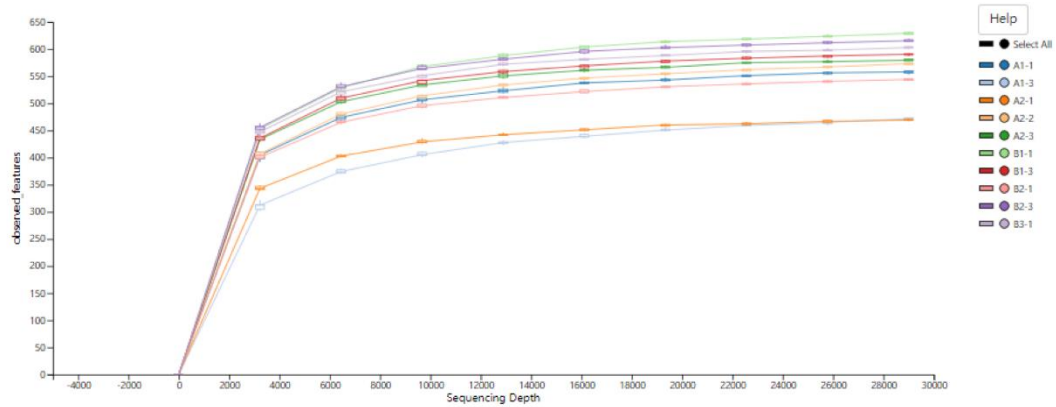
12 Supplementary Figures



28

29 **Supplementary Figure 1** Details of sampling and analysis. Circles represent sampling

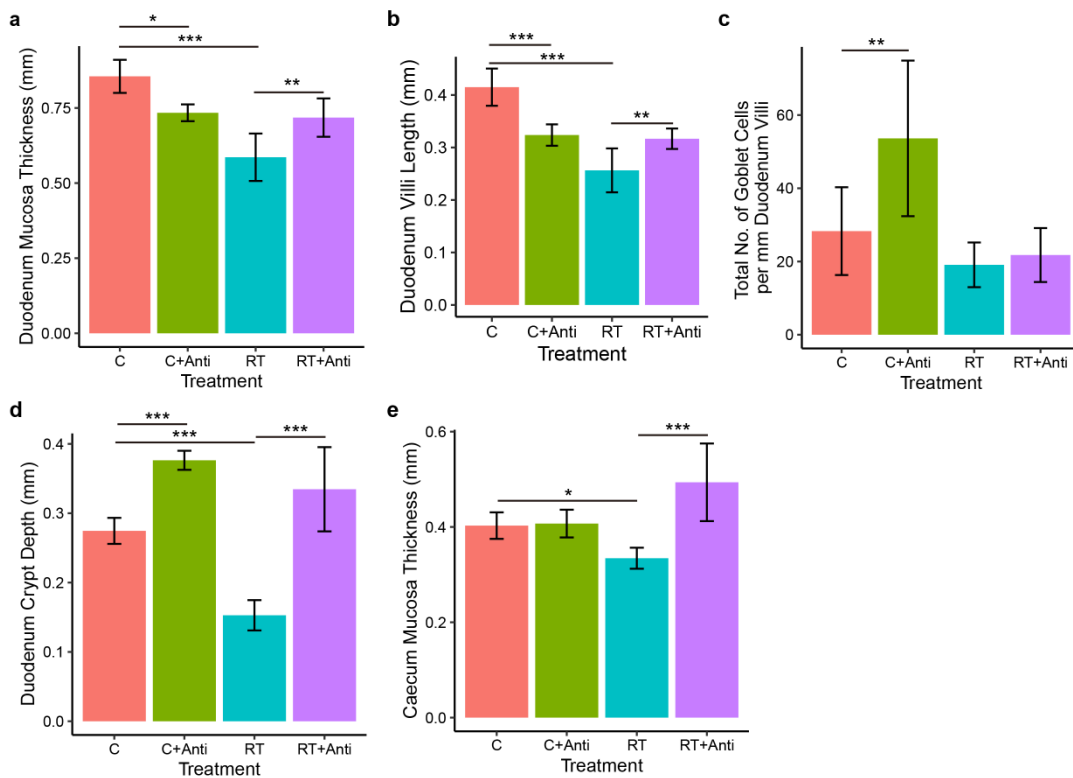
30 types and analysis items; forks indicate that the corresponding items were not analyzed.



31

32 **Supplementary Figure 2** Rarity curves for 86 samples.

33



34

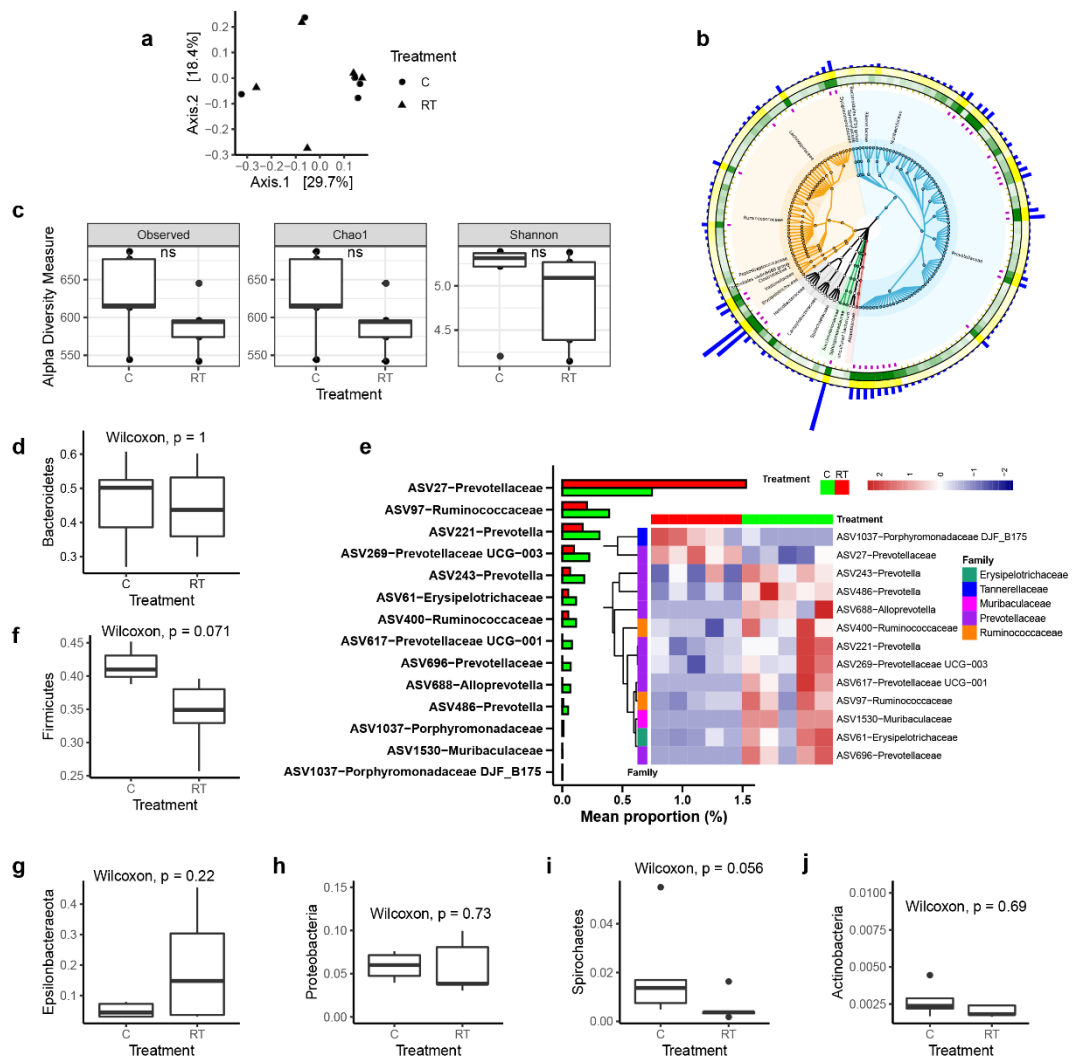
35 **Supplementary Figure 3** Cold-exposed piglets show an increased index for the

36 duodenum. **a** Duodenal mucosa thicknesses. **b** Duodenal villus length. **c** Total number

37 of goblet cells per mm duodenal villi. **d** Duodenal crypt depth. **e** Cecal mucosa

38 thickness. The data are the means \pm SEMs. Statistical significance was determined

39 using Wilcoxon test (* $p < 0.05$, ** $p < 0.01$, *** $p < 0.001$).

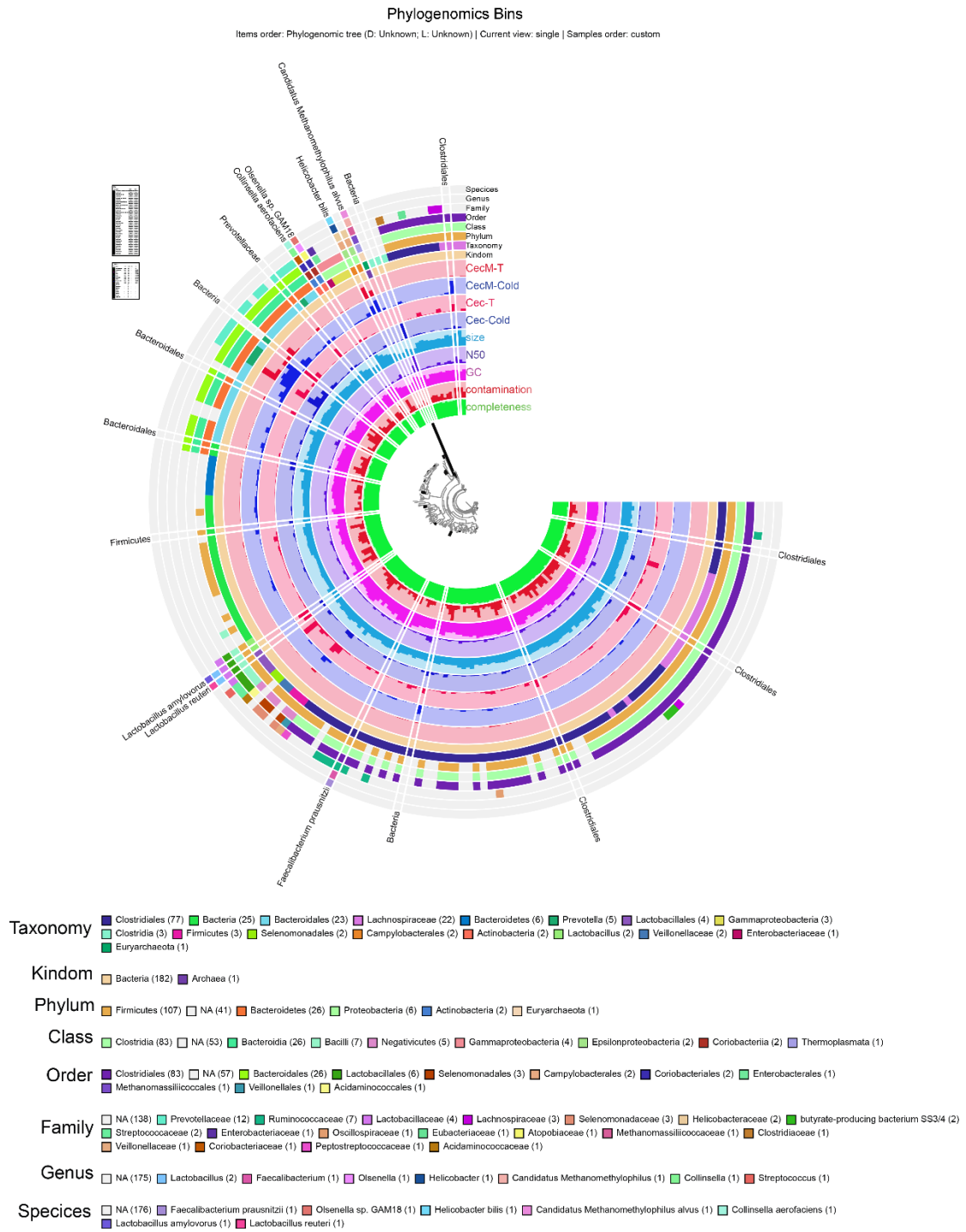


40

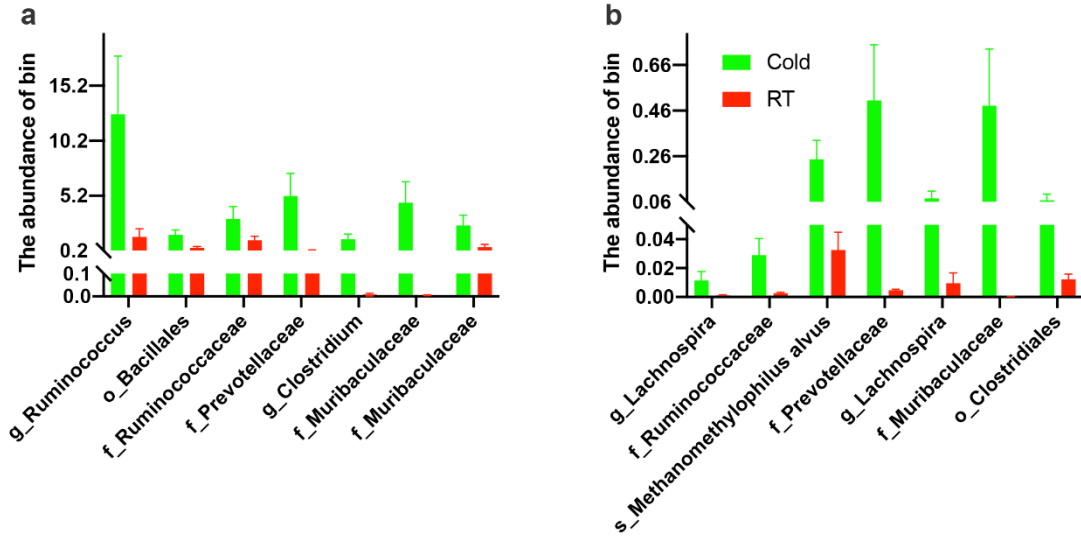
41 **Supplementary Figure 4** Cold exposure changes the composition of the epithelial
 42 surface of the cecum. **a** Principal coordinates analysis (PCoA) based on weighted
 43 UniFrac analysis. Each symbol represents a single sample of cecal content after 48 h of
 44 cold stress (n = 5) or RT (n = 5 per group). **b** Heatmap tree comparing the most abundant
 45 ASVs from the cecal content of 48 h cold-stressed animals (n = 5, inner green rings)
 46 and RT controls (n = 5, outer yellow rings) and their phylogenetic relationships. The
 47 bar represents abundant ASVs. **c** Alpha diversity of ASVs. **d** Boxplot of the microbiota
 48 of the cecal content at the phylum level. **e** The different ASVs with bars and heatmaps
 49 with $P < 0.05$. **f-j** Boxplot of the microbiota of the cecal content at the phylum level.

50 The data are the means \pm SEMs. Statistical significance was determined using Wilcoxon
 51 test ($*p < 0.05$, $**p < 0.01$, $***p < 0.001$).

52

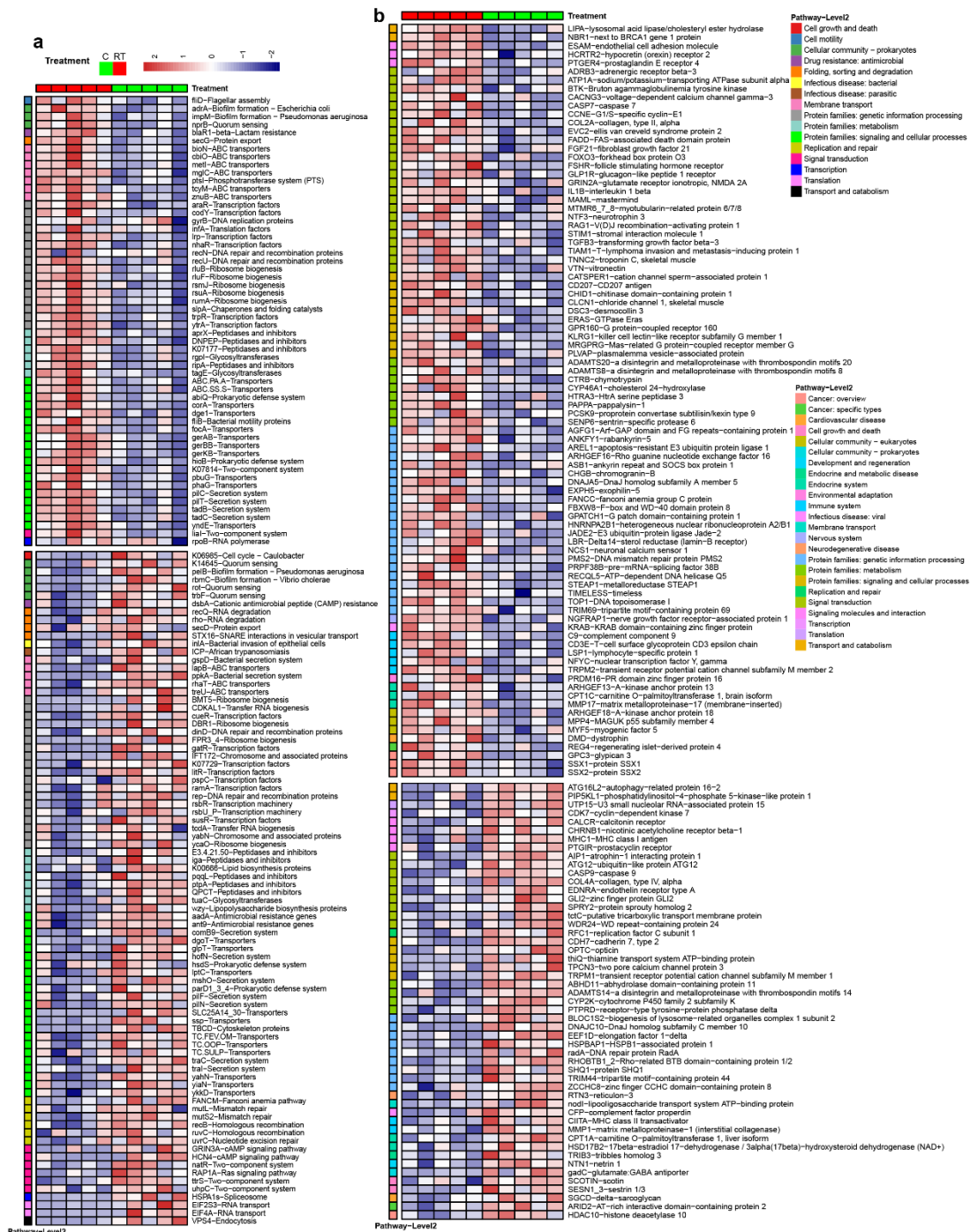


54 **Supplementary Figure 5** Phylogenomic tree with 191 bins with a completeness $\geq 90\%$
 55 and contamination $\leq 5\%$.

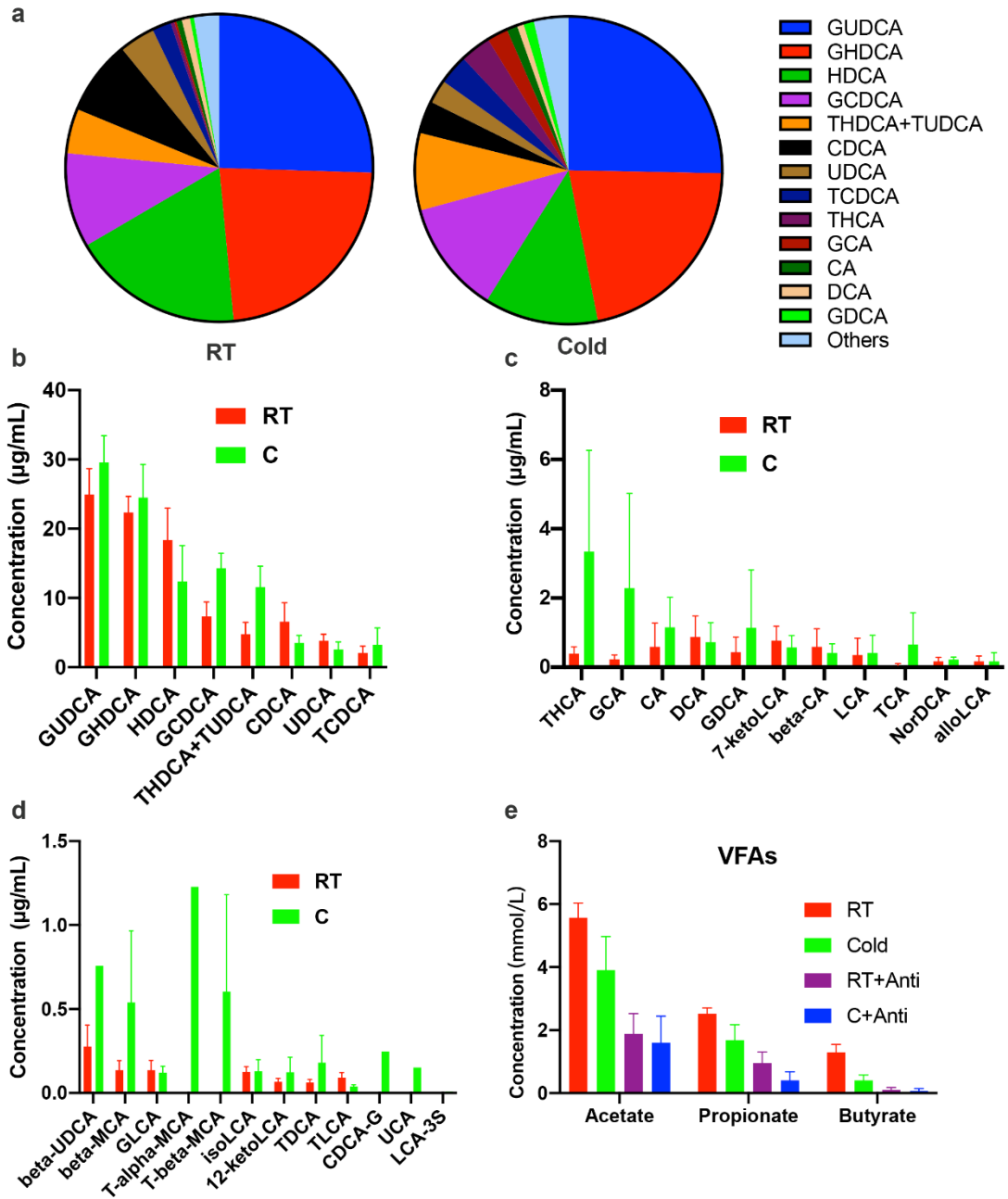


56

57 **Supplementary Figure 6** Significant bins after STAMP analysis between the RT and
 58 cold-stressed groups. The different bins **(a)** in the content and **(b)** on the epithelial
 59 surface of the cecum.



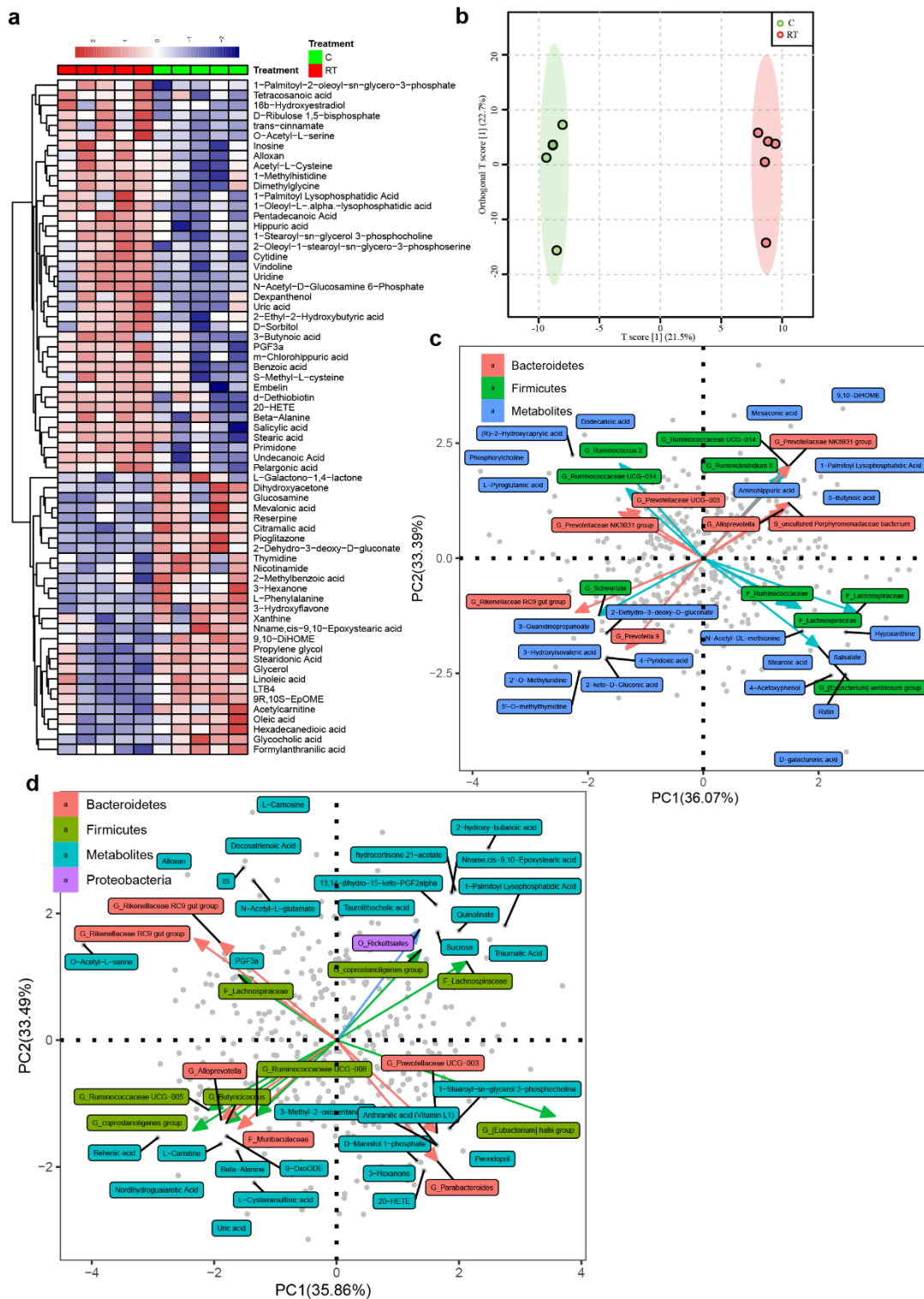
Supplementary Figure 7 Cold exposure changes other functions of the microbiota in the cecum. Heatmap of the differences in the microbiota in the cecum at other functional levels (a) in the content and (b) on the epithelium surface of the cecum.



64

65 **Supplementary Figure 8** Cold exposure changes bile acid concentrations in serum (**a-**

66 **d**) and SCFA levels (**e**) in the cecal content.



67

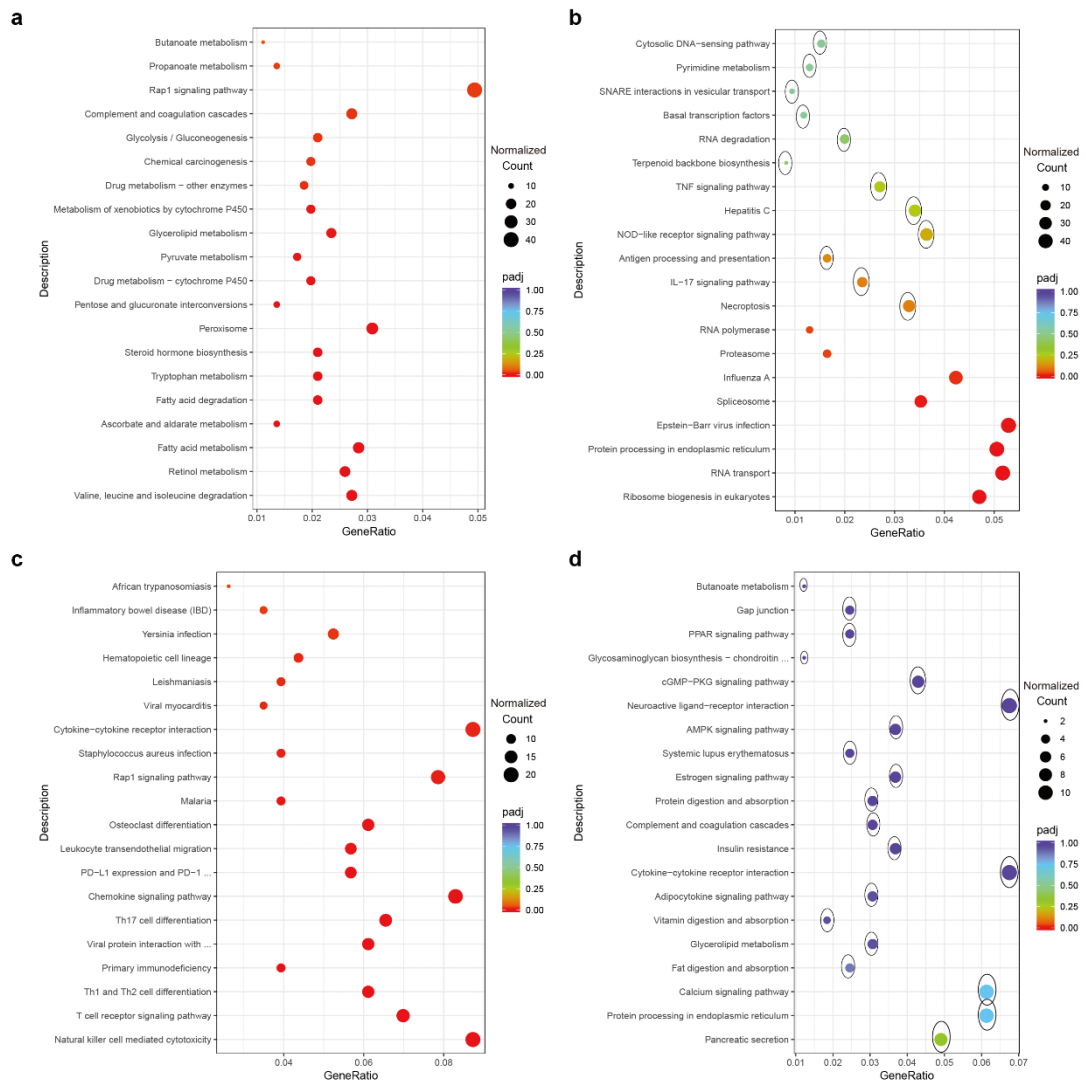
68 **Supplementary Figure 9** Different metabolomic alterations in the negative model in

69 serum and strong correlation with the microbiome of the contents and epithelial surface

70 of the cecum. **a** Heatmap of the differences in serum metabolomic metabolites under

71 cold stress. **b** Partial least-squares discriminant analysis (PLS-DA) of microbial
 72 metabolites in serum. **c** Correlation of the metabolites in serum with the microbiome of
 73 the cecal contents. **d** Correlation of the metabolites with the microbiome of the
 74 epithelial surface of the cecum.

75

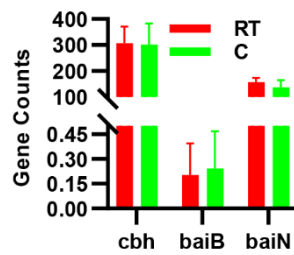


76

77 **Supplementary Figure 10** Summary of pathways identified at the RNA expression
78 level by RNA seq. **a** Downregulated pathways under cold stress compared with RT in
79 the liver of piglets. **b** Upregulated pathways under cold stress compared with RT in
80 the liver of piglets. **c** Downregulated pathways under cold stress compared with RT in
81 the fat of piglets. **d** Upregulated pathways under cold stress compared with RT in the
82 fat of piglets. The circled nodes indicate results that are not significant ($p_{adj} > 0.05$),
83 and unmarked nodes show significant findings ($p_{adj} < 0.05$).

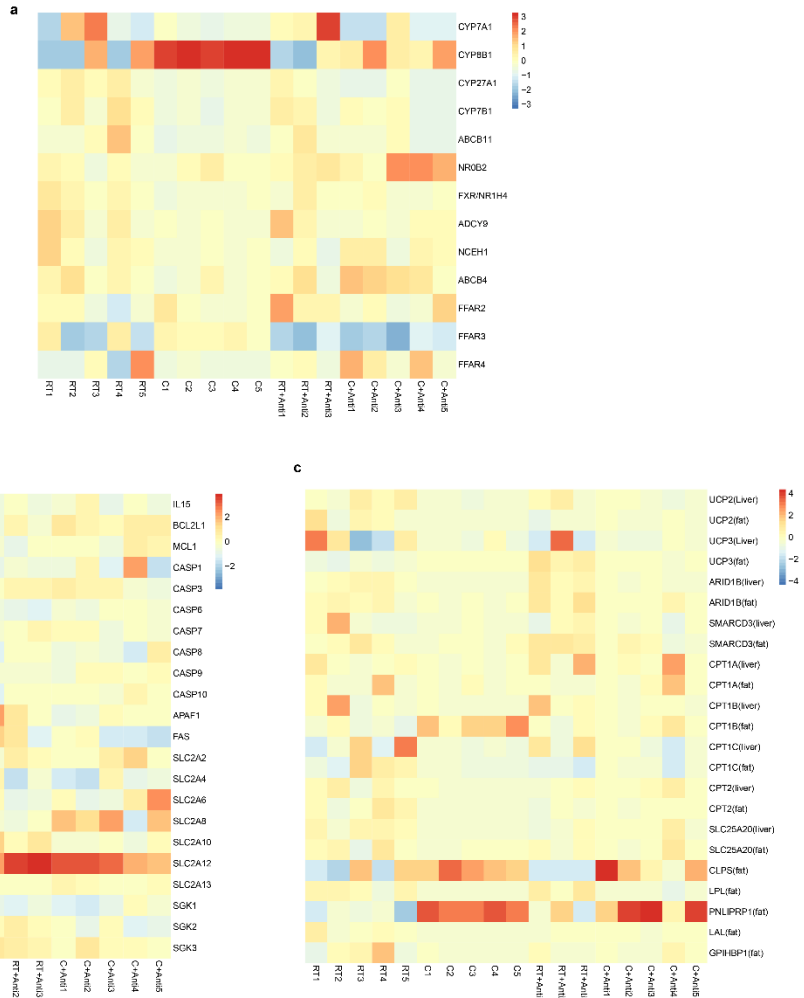
84

85



86

87 **Supplementary Figure 11** The counts of genes involved in secondary bile acid
88 biosynthesis in the gut microbiota of the cecum content by metagenomic sequencing.
89 Cbh, conjugated bile acid hydrolase, baiB, bile acid-coenzyme A ligase, baiN, 3-
90 dehydro-bile acid delta (4,6)-reductase.



91

92 **Supplementary Figure 12** Heatmaps showing the variability between samples, **(a, b,**

93 **c)** related to Figure 6.